diversity

MDPI

Article

Multi-Gene Phylogeny and Taxonomy of *Hypoxylon* (Hypoxylaceae, Ascomycota) from China

Haixia Ma [1,2,3,*,†], Zikun Song [1,4,†], Xiaoyan Pan [1,5], Yu Li [4], Zhanen Yang [1,6], Zhi Qu [1]

[1] Institute of Tropical Bioscience and Biotechnology, Chinese Academy of Tropical Agricultural Sciences, Haikou 571101, China; michellesong2021@yeah.net (Z.S.); pxy960501@yeah.net (X.P.); fungizhaneny@163.com (Z.Y.); quzhi@itbb.org.cn (Z.Q.)
[2] Hainan Institute for Tropical Agricultural Resources, Chinese Academy of Tropical Agricultural Sciences, Haikou 571101, China
[3] Hainan Key Laboratory of Tropical Microbe Resources, Haikou 571101, China
[4] College of Plant Protection, Jilin Agricultural University, Changchun 130000, China; yuli966@126.com
[5] College of Forestry, Hainan University, Haikou 571101, China
[6] College of Biodiversity Conservation, Southwest Forestry University, Kunming 650224, China
* Correspondence: mahaixia@itbb.org.cn
† Haixia Ma and Zikun Song contributed equally to this work.

Abstract: The *Hypoxylon* species play an important ecological role in tropical rainforest as wood-decomposers, and some might have benefical effects on their hosts as endophytes. The present work concerns a survey of the genus *Hypoxylon* from Hainan Tropical Rainforest National Park of China. Four new species: *H. wuzhishanense*, *H. hainanense*, *H. chrysalidosporum*, and *H. cyclobalanopsidis*, were discovered based on a combination of morphological characteristics and molecular data. *Hypoxylon wuzhishanense* is characterized by Rust pulvinate stromata, amyloid apical apparatus and brown ascospores, with most of the perispore being indehiscent in 10% KOH. *Hypoxylon hainanense* has effused–pulvinate and Violet stromata, amyloid apical apparatus, light-brown to brown ascospores with straight germ slit and dehiscent perispore. *Hypoxylon chrysalidosporum* is distinguished by glomerate to pulvinate stromata, highly reduced or absent inamyloid apical apparatus, and light-brown to brown ascospores with very conspicuous coil-like ornamentation. *Hypoxylon cyclobalanopsidis* has Livid Purple pulvinate stromata, highly reduced amyloid apical apparatus, faint bluing, brown ascospores and dehiscent perispore, and it grows on dead branches of *Cyclobalanopsis*. Detailed descriptions, illustrations, and contrasts with morphologically similar species are provided. Phylogenetic analyses inferred from ITS, RPB2, LSU, and β-tubulin sequences confirmed that the four new species are distinct within the genus *Hypoxylon*.

Keywords: Ascomycota; molecular phylogenetics; wood-decomposing fungi; tropical rainforest; taxonomy; *Hypoxylon*; Hainan Tropical Rainforest National Park

Citation: Ma, H.; Song, Z.; Pan, X.; Li, Y.; Yang, Z.; Qu, Z. Multi-Gene Phylogeny and Taxonomy of *Hypoxylon* (Hypoxylaceae, Ascomycota) from China. *Diversity* **2022**, *14*, 37. https://doi.org/10.3390/d14010037

Academic Editor: Ipek Kurtboke

Received: 1 December 2021
Accepted: 4 January 2022
Published: 7 January 2022

1. Introduction

Hypoxylon Bull., described by Bulliard in 1791 [1], is a genus that contains primarily saprotrophs and endophytes of angiospermous plants [2,3]. The genus *Hypoxylon*, together with *Annulohypoxylon* Y.M. Ju, J.D. Rogers, H.M. Hsieh and *Daldinia* Ces., De Not., are all closely associated with both dicots and, infrequently, monocots in forest ecosystems [4]. Most hypoxylaceous fungi have a strong capacity to degrade cellulose and lignin and are important elements in forest ecosystems, playing a key ecological role in carbon circulation [5]. In addition, the endophytic stages of these fungi may even benefit their host plants by protecting them from pathogens [6,7].

The type genus *Hypoxylon* is the largest genus in the Hypoxylaceae, with more than 200 species [8] and 1173 epithets in the Index Fungorum

(http://www.indexfungorum.org/names/names.asp, accessed on 1 November 2021). Members of the genus have a world-wide distribution, but they display a higher diversity in the tropics and subtropics [4,6,9,10]. In the 20th century, the generic concept of *Hypoxylon* was based only on morphological characteristics [1,4,11–15]. Currently, morphological, phylogenetic, and chemotaxonomic evidence, has also been used to infer species limits in inter- and intra-genera in Hypoxylaceae [3,6,10] and to segregate some new genera such as *Annulohypoxylon* [16], *Hypomontagnella* [17], *Jackrogersella*, and *Pyrenopolyporus* [18] from the genus *Hypoxylon*. The genus *Hypoxylon* is quite common in China; however, the occurrence of the species in China has not been confirmed by molecular phylogenetic analyses, and the species diversity and distribution of the genus in China are unclear [19–22].

Hainan Tropical Rainforest National Park is located in south-central Hainan province, between 18°33′16″–19°14′16″ N and 108°44′32″–111°04′43″ E and has a tropical monsoon climate. More than 3577 plant species, 1142 genera, and 220 families have been reported in the rainforest park (http://www.hntrnp.com, accessed on 15 November 2021), including abundant hypoxylaceous fungi. During investigations on Xylariales from Hainan Province, China, some specimens of Hypoxylaceae were collected. These collections were carefully studied using both morphological and phylogenetic methods, and four undescribed species of *Hypoxylon* were identified. The aims of this study were to confirm the taxonomic status of the new species, explore the species diversity of *Hypoxylon* in Hainan Tropical Rainforest National Park, and infer the evolutionary relationships of the genus *Hypoxylon*.

2. Materials and Methods

2.1. Sample Sources

The studied specimens were collected from Hainan Tropical Rainforest National Park, China, in 2020. These specimens were deposited at the Fungarium of the Institute of Tropical Bioscience and Biotechnology, Chinese Academy of Tropical Agricultural Sciences (FCATAS).

2.2. Morphological Characterization

The micromorphological observations, micrographs, and measurements were obtained using an Olympus IX73 inverted fluorescence microscope (Tokyo, Japan) with the laser capture microdissection system of model MMI CellCut Plus (Zurich, Switzerland), while the same processes for observing the morphological characteristics of stromatal sufaces and perithecia were performed using a VHX-600E microscope from the Keyence Corporation. The photographs of ascospores were examined by scanning electron microscope (SEM) (Hitachi Corporation, Tokyo, Japan). Sexual structures were microscopically observed in water, 10% KOH, and Melzer's reagent, as determined by Ju and Rogers [4]. The color codes appearing in this article refer to Rayner [23]. In the text, the following abbreviations are used: KOH = 10% potassium hydroxide, n = number of ascospores measured from a given number of specimens, M = arithmetical average of sizes of all ascospores.

2.3. DNA Extraction, PCR Amplification, and Sequencing

Following the instructions of the manufacturer, total genomic DNA of studied samples was extracted using an improved cetyltrimethylammonium bromide (CTAB) rapid extraction kit for plant genomes (Aidlab Biotechnologies, Beijing, China) and a Thermo Scientific Phire Plant Direct PCR Kit (Thermo Fisher Scientific, Waltham, MA, USA). Four DNA loci of ITS (internal transcribed spacer regions), nLSU (nuclear large subunit ribosomal DNA), RPB2 (RNA polymerase II second largest subunit), and β-tubulin (beta-tubulin) were amplified by polymerase chain reaction (PCR) using HS Taq Mix (Dongsheng Biotech, Guangzhou, China). The 40 μL PCR mixtures contained 16 μL of ddH2O, 20 μL of 2 × HS™ Mix, 2 μL of DNA template, and 1 μL of each forward and reverse primer. The

primer pairs ITS5/ITS4, LR0R/LR5, fRPB2-7CR/fRPB2-5F, and T1/T22 were used to amplify ITS, LSU, RPB2, and β-tubulin, respectively [24–28]. The PCR thermal cycling program for ITS was set as initial denaturation at 95 °C for 3 min, followed by 30 cycles of denaturation at 94 °C for 40 s, annealing at 55.8 °C for 45 s, extension at 72 °C for 1 min, and a final extension at 72 °C for 10 min. For generation of LSU sequence data, the following program was used: initial denaturation at 94 °C for 3 min, 36 cycles of 1 min at 94 °C, 50 s at 52 °C and 1 min at 72 °C, with a final extension period of 10 min at 72 °C. The PCR amplification of RPB2 and β-tubulin was set up as follows: initial denaturation at 95 °C for 3 min, followed by 35 cycles at 94 °C for 1 min, 52 °C for 50 s, 72 °C for 1 min, with a final extension of 72 °C for 10 min [29]. PCR sample purification and DNA sequencing were carried out by BGI, Guangzhou, China. The generated sequences were submitted to GenBank to acquire accession numbers.

2.4. Phylogenetic Analysis

All newly generated sequences and relevant sequences of closely related species within the genus *Hypoxylon* and among genera of the family Hypoxylaceae and some related genera of the Xylariales based on ITS, LSU, RPB2, and β-tubulin were obtained in the phylogenetic analysis (Table 1). The other genera included *Annulohypoxylon*, *Daldinia*, *Hypomontagnella*, *Jackrogersella*, *Pyrenopolyporus, Rhopalostroma*, and *Thamnomyces*. The phylogenetic trees were rooted with *Xylaria hypoxylon* (L.) Grev. and *Biscogniauxia nummularia* (Bull.) Kuntze as outgroups.

Table 1. A list of species, specimen numbers, locality, GenBank accession numbers, and references used in this study. Holotype and epitype specimens are labelled as T and ET respectively. Species highlighted in bold were derived from this study. N/A: not available.

Species Name	Specimen No.	Locality	GenBank Accession No.				Status	Reference
			ITS	LSU	RPB2	β-tubulin		
Annulohypoxylon annulatum	CBS 140775	USA	KU604559	KY610418	KY624263	KX376353	ET	[10,18,30]
A. moriforme	CBS 123579	Martinique	KX376321	KY610425	KY624289	KX271261		[30]
A. truncatum	CBS 140778	USA	KX376329	KY610419	KY624277	KX376352	ET	[18,30]
Daldinia dennisii	CBS 114741	Australia	JX658477	KY610435	KY624244	KC977262	T	[6,18,31]
D. petriniae	MUCL 49214	Austria	JX658512	KY610439	KY624248	KC977261	ET	[6,18,31]
Hypomontagnella barbarensis	STMA 14081	Argentina	MK131720	MK131718	MK135891	MK135893	T	[17]
Hypom. monticulosa	MUCL 54604	French Guiana	KY610404	KY610487	KY624305	KX271273	ET	[18]
Hypom. submonticulosa	CBS 115280	France	KC968923	KY610457	KY624226	KC977267		[6,18]
Hypoxylon anthochroum	YMJ 9	Mexico	JN660819	N/A	N/A	AY951703		[16]
H. aveirense	CMG 29	Portugal	MN053021	N/A	N/A	MN066636	T	[32]
H. begae	YMJ 215	USA	JN660820	N/A	N/A	AY951704		[16]
H. brevisporum	YMJ 36	Puerto Rico	JN660821	N/A	N/A	AY951705		[16]
H. carneum	MUCL 54177	France	KY610400	KY610480	KY624297	KX271270		[18]
H. cercidicola	CBS 119009	France	KC968908	KY610444	KY624254	KX271270		[6,18]
H. chrysalidosporum	**FCATAS2710**	**China**	**OL467294**	**OL615106**	**OL584222**	**OL584229**	**T**	**This study**
H. chrysalidosporum	**FCATAS2711**	**China**	**OL467295**	**OL615107**	**OL584223**	**OL584230**		**This study**
H. crocopeplum	CBS 119004	France	KC968907	KY610445	KY624255	KC977268		[18]
H. cyclobalanopsidis	**FCATAS2714**	**China**	**OL467298**	**OL615108**	**OL584225**	**OL584232**	**T**	**This study**
H. cyclobalanopsidis	**FCATAS2715**	**China**	**OL467299**	**OL615109**	**OL584226**	**OL584233**		**This study**

H. dieckmannii	YMJ 89041203	China	JN979413	N/A	N/A	AY951713		[16]
H. duranii	YMJ 85	China	JN979414	N/A	N/A	AY951714		[16]
H. erythrostroma	YMJ 90080602	China	JN979416	N/A	N/A	AY951716		[16]
H. eurasiaticum	MUCL 57720	Iran	MW367851	N/A	MW373852	MW373861		[33]
H. fendleri	DSM 107927	USA	MK287533	MK287545	MK287558	MK287571		[34]
H. ferrugineum	CBS 141259	Austria	KX090079	N/A	N/A	KX090080		[35]
H. fragiforme	MUCL 51264	Germany	KM186294	KM186295	KM186296	KM186293	ET	[36]
H. fraxinophilum	MUCL 54176	France	KC968938	N/A	N/A	KC977301	ET	[6]
H. fulvosulphureum	MFLUCC 13-0589	Thailand	KP401576	N/A	N/A	KP401584	T	[37]
H. fuscum	CBS 113049	France	KY610401	KY610482	KY624299	KX271271	ET	[18]
H. griseobrunneum	CBS 331.73	India	KY610402	MH872399	KY624300	KC977303	T	[6,18,38]
H. guilanense	MUCL 57726	Iran	MT214997	MT214992	MT212235	MT212239	T	[8]
H. haematostroma	MUCL 53301	Martinique	KC968911	KY610484	KY624301	KC977291	ET	[6,18]
H. hainanense	**FCATAS2712**	**China**	**OL467296**	**OL616132**	**OL584224**	**OL584231**	**T**	**This study**
H. hainanense	**FCATAS2713**	**China**	**OL467297**	**N/A**	**N/A**	**N/A**		**This study**
H. hinnuleum	MUCL 3621	USA	MK287537	MK287549	MK287562	MK287575	T	[36]
H. howeanum	MUCL 47599	Germany	AM749928	KY610448	KY624258	KC977277		[6,18,39]
H. hypomiltum	MUCL 51845	Guadeloupe	KY610403	KY610449	KY624302	KX271249		[18]
H. invadens	MUCL 51475	France	MT809133	MT809132	MT813037	MT813038	T	[40]
H. investiens	CBS 118183	Malaysia	KC968925	KY610450	KY624259	KC977270		[6,18]
H. isabellinum	STMA10247	Martinique	STMA10247	N/A	N/A	KC977295	T	[6]
H. jaklitschii	JF 13037	Sri Lanka	KM610290	N/A	N/A	KM610304	T	[41]
H. lateripigmentum	MUCL 53304	Martinique	KC968933	KY610486	KY624304	KC977290	T	[6,18]
H. lenormandii	CBS 135869	Cameroon	KY610390	KY610453	KY624262	KM610295		[18,41]
H. liviae	CBS 115282	Norway	NR155154	N/A	N/A	KC977265	ET	[6]
H. lividicolor	YMJ 70	China	JN979432	N/A	N/A	AY951734		[16]
H. lividipigmentum	YMJ 233	Mexico	JN979433	N/A	N/A	AY951735		[16]
H. macrosporum	YMJ 47	Canada	JN979434	N/A	N/A	AY951736		[16]
H. musceum	MUCL 53765	Guadeloupe	KC968926	KY610488	KY624306	KC977280		[6,18]
H. notatum	YMJ 250	USA	JQ009305	N/A	N/A	AY951739		[16]
H. olivaceopigmentum	DSM 10792	USA	MK287530	MK287542	MK287555	MK287568	T	[34]
H. papillatum	ATCC 58729	USA	NR155153	KY610454	KY624223	KC977258	T	[6,18]
H. perforatum	CBS 115281	France	KY610391	KY610455	KY624224	KX271250		[18]
H. petriniae	CBS 114746	France	NR155185	KY610491	KY624279	KX271274	T	[18]
H. pilgerianum	STMA 13455	Martinique	KY610412	N/A	KY624308	KY624315		[18]
H. porphyreum	CBS 119022	France	KC968921	KY610456	KY624225	KC977264		[6,18]
H. pseudofendleri	MFLUCC 11-0639	Thailand	KU940156	KU863144	N/A	N/A		[42]
H. pseudofuscum	18264	Germany	MW367857	MW367848	MW373858	MW373867	T	[33]
H. pulicicidum	CBS 122622	Martinique	JX183075	KY610492	KY624280	JX183072	T	[18,43]
H. rickii	MUCL 53309	Martinique	KC968932	KY610416	KY624281	KC977288	ET	[18]
H. rubiginosum	MUCL 52887	Germany	KC477232	KY610469	KY624266	KY624311	ET	[18,44]
H. samuelsii	MUCL 51843	Guadeloupe	KC968916	KY610466	KY624269	KC977286	ET	[6,18]
H. shearii	YMJ 29	Mexico	EF026142	N/A	N/A	AY951753		[16]
H. spegazzinianum	STMA 14082	Argentina	KU604573	N/A	N/A	KU604582	T	[10]

H. sporistriatatunicum	UCH9542	Panama	MN056426	N/A	N/A	MK908140	T	[45]
H. subgilvum	YMJ 88113007	China	JQ009315	N/A	N/A	AY951755		[16]
H. sublenormandii	JF 13026	Sri Lanka	KM610291	N/A	N/A	KM610303	T	[41]
H. teeravasati	PUFD 4	India	N/A	MF385274	MG986895	MG986894		[46]
H. texense	DSM 107933	USA	MK287536	MK287548	MK287561	MK287574	T	[34]
H. trugodes	MUCL 54794	Sri Lanka	KF234422	NG066380	KY624282	KF300548	ET	[6,18]
H. ulmophilum	YMJ 350	Russia	JQ009320	N/A	N/A	AY951760		[16]
H. vogesiacum	CBS 115273	France	KC968920	KY610417	KY624283	KX271275		[18]
H. wuzhishanense	**FCATAS2708**	**China**	**OL467292**	**OL615104**	**OL584220**	**OL584227**	**T**	**This study**
H. wuzhishanense	**FCATAS2709**	**China**	**OL467293**	**OL615105**	**OL584221**	**OL584228**		**This study**
Jackrogersella cohaerens	CBS 119126	Germany	KY610396	KY610497	KY624270	KY624314		[18]
J. multiformis	CBS 119016	Germany	KC477234	KY610473	KY624290	KX271262	ET	[6,18]
Pyrenopolyporus hunteri	MUCL 52673	Ivory Coast	KY610421	KY610472	KY624309	KU159530	ET	[18,30]
P. laminosus	MUCL 53305	Martinique	KC968934	KY610485	KY624303	KC977292	T	[6,18]
P. nicaraguensis	CBS 117739	Burkina Faso	AM749922	KY610489	KY624307	KC977272		[6,18,39]
Rhopalostroma angolense	CBS 126414	Ivory Coas	KY610420	KY610459	KY624228	KX271277		[18]
Thamnomyces dendroidea	CBS 123578	French Guiana	FN428831	KY610467	KY624232	KY624313	T	[18,47]
Xylaria hypoxylon	CBS 122620	Sweden	KY610407	KY610495	KY624231	KX271279	ET	[18]
Biscogniauxia nummularia	MUCL 51395	France	KY610382	KY610427	KY624236	KX271241		[18]

The sequence alignment was conducted using fast Fourier transformation (MAFFT) online (http://mafft.cbrc.jp/alignment/server/, accessed on 22 November 2021) [48]. Further sequence processing was conducted using BioEdit 7.0.5, and the concatenation of four DNA loci of ITS, LSU, RPB2, and β-tubulin was completed using MEGA 6.0 [29,49,50].

A combined matrix of ITS–LSU–RPB2–β-tubulin was used to construct phylogenetic trees and analyzed by two methods: Maximum Likelihood (ML) and Bayesian Inference (BI). Maximum Likelihood (ML) analysis was performed using raxmlGUI 2.0 with rapid bootstrap search executing 1000 replicates, setting the substitution model as GTR-GAMMA+G [45,51]. Bayesian analysis was performed using MrBayes v.3.2.6, based on using jModelTest 2 to conduct model discrimination [52]. The selected applicable model implemented the Markov Chain Monte Carlo (MCMC) algorithm, which determined posterior probabilities (PP) [53]. Six simultaneous Markov chains were run for 1000000 generations, from which every 100th generation was sampled as a tree [54–58]. Phylogenetic trees were viewed in FigTree 1.4.2 [59]. The phylogenetic tree and multi-gene sequence alignment were deposited in TreeBASE (www.treebase.org/treebase-web/home.html, accessed on 20 December 2021) with accession number S29126.

3. Results

3.1. Phylogenetic Analysis

The sequence datasets for the contributions of the molecular phylogenetic trees consisted of 82 ITS, 57 LSU, 58 RPB2, and 81 β-tubulin sequences. All of the 278 sequences came from 79 strains including 4 newly described *Hypoxylon* taxa, 58 known *Hypoxyplon* taxa, 3 *Annulohypoxylon* taxa, 2 *Daldinia* taxa, 3 *Hypomontagnella* taxa, 2 *Jackrogersella* taxa, 3 *Pyrenopolyporus* taxa, 1 *Rhopalostroma* taxon and 1 *Thamnomyces* taxon, as well as the *X. hypoxylon* and *B. nummularia* as outgroups.

After aligned by MAFFT online, the sequence datasets contained 2046 character positions for ITS alignment, 3320 character positions for LSU alignment, 1285 character positions for RPB2 alignment, and 2298 character positions for β-tubulin alignment. With

less informative positions trimmed, and four DNA loci connected, the generated multi-gene alignment (MGA) had an aligned length of 3836 characters, of which 1977 characters were parsimony-informative. Phylogenetic trees generated from BI and ML analyses of the combined dataset of ITS–LSU–RPB2–β-tubulin were highly similar in topology. Only the ML tree is shown in Figure 1, with ML bootstrap values ≥ 50% and Bayesian posterior probabilities ≥ 0.95 labelled along the branches.

The phylogenies reveal a paraphyly of *Hypoxylon*, with the genera *Annulohypoxylon*, *Daldinia*, *Hypomontagnella*, *Jackrogersella*, *Pyrenopolyporus*, and *Thamnomyces* embedded within the former. The phylogeny inferred from the ITS–LSU–RPB2–β-tubulin sequences demonstrated that the four new species, i.e., *H. wuzhishanense*, *H. hainanense*, *H. chrysalidosporum*, and *H. cyclobalanopsidis*, formed distinct well-supported lineages (Figure 1).

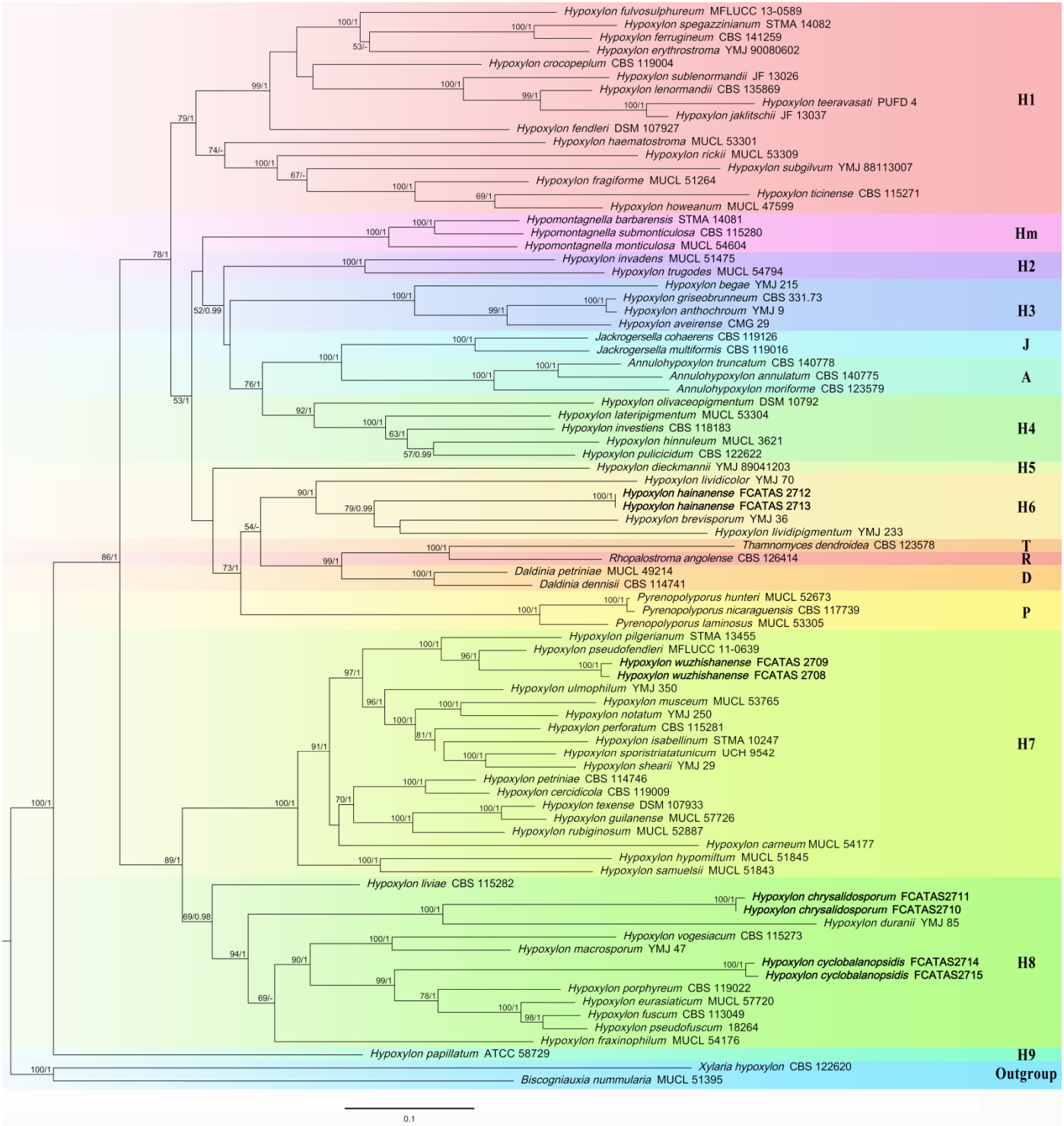

Figure 1. ML phylogram of the *Hypoxylon* species based on the multi-gene alignment of ITS–LSU–RPB2–β-tubulin. Support values of ML and BI analyses (bootstrap support ≥ 50%, posterior probabilities value ≥ 0.95) are labelled above or below the respective branches (ML/BI). New species are labelled in bold.

3.2. Taxonomy

Hypoxylon chrysalidosporum Hai X. Ma, Z.K. Song, sp. nov., Figure 2.

MycoBank: MB 841956.

Diagnosis. Differs from *H. duranii* and *H. notatum* in its KOH-extractable pigments, highly reduced or absent inamyloid apical apparatus, and smaller ascospores with straight germ slit.

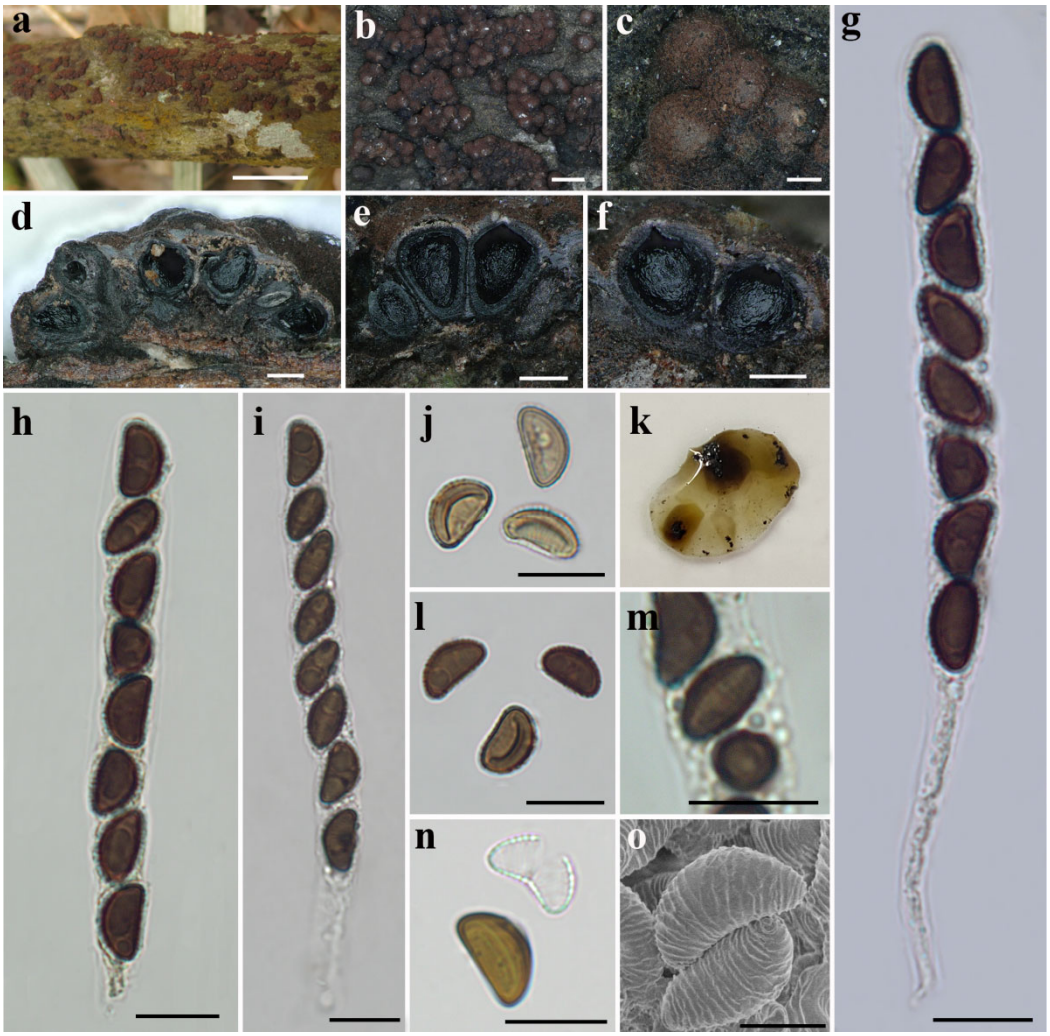

Figure 2. *Hypoxylon chrysalidosporum* (holotype FCATAS 2710). (**a**) Stromata on dead corticated branch. (**b**,**c**) Stromatal surface. (**d**–**f**) Stroma in vertical section showing the perithecia and tissue below the perithecial layer. (**g**,**h**) Ascus in Melzer's reagent. (**i**) Ascus in water. (**j**,**l**) Ascospore in water. (**k**) KOH-extractable pigments. (**m**) Ascospores in Melzer's reagent showing germ slit. (**n**) Ascospores in 10% KOH. (**o**) Ascospore under SEM. Scale bars: (**a**) = 1cm; (**b**) = 1 mm; (**c**–**f**) = 200 μm; (**g**–**j**,**l**–**n**) = 10 μm; (**o**) = 5 μm.

Etymology. *Chrysalidosporum* (Lat.): referring to the chrysalis-shaped ascospores.

Holotype. CHINA: Hainan Province, Ledong County, Hainan Tropical Rainforest National Park, Jianfengling National Natural Reserve, approximately 108°51′ E and 18°47′ N, elevation approximately 700 m, saprobic on surface of dead corticated branches, 24 October 2020, Haixia Ma, Col. J214 (FCATAS 2710).

Teleomorph. Stromata glomerate to effused–pulvinate, with conspicuous perithecial mounds, 0.1–0.7 cm long × 0.1–0.3 cm broad × 0.3–0.5 mm thick; surface Bay (6), Rust (39), Dark Brick (60) and Livid Purple (81); with pale brown to dull reddish brown granules immediately beneath the surface and between perithecia; yielding Pale Luteous (11), Honey (60) and Ochreous (44) pigments in 10% KOH; tissue below the perithecial layer black, inconspicuous, 0.1–0.4 mm thick. Perithecia spherical to obovoid, black, 0.2–0.4 mm broad × 0.3–0.4 mm high. Ostioles umbilicate, encircled with a paler area, opening lower than the stromatal surface. Asci cylindrical, eight-spored, uniseriate, 75–139 μm total length × 6.6–11.9 μm broad; the spore-bearing portion 49–82 μm long, and stipes 19–71 μm long, with inamyloid apical apparatus highly reduced or absent, not bluing in Melzer's reagent. Ascospores light-brown to brown, unicellular, ellipsoid-inequilateral, with slightly broad rounded ends, 8–10.6(–11.1) × 4.1–6.3(–7.1) μm (n = 60, M = 9.2 × 5.3 μm), with

conspicuously straight spore-length germ slit on the convex side; perispore dehiscent in 10% KOH, with very conspicuous coil-like ornamentation in SEM; epispore smooth.

Additional specimens examined. CHINA: Hainan Province, Ledong County, Hainan Tropical Rainforest National Park, Jianfengling National Natural Reserve, approximately 108°49′ E and 18°50′ N, elevation approximately 750 m, saprobic on surface of dead corticated branches, 24 October 2020, Haixia Ma, Col. J1059 (FCATAS 2711).

Hypoxylon cyclobalanopsidis Hai X. Ma, Z.K. Song, sp. nov., Figure 3.
MycoBank: MB 841957.

Diagnosis. Differs from *H. porphyreum* in its larger ascospores, KOH-extractable pigments, host plant and distribution. Differs from *H. eurasiaticum*, *H. fuscum*, and *H. pseudofuscum* in its smaller apical apparatus, host plant and tropical distribution.

Etymology. *Cyclobalanopsidis* (Lat.): referring to the host genus *Cyclobalanopsis* which the fungus inhabits.

Holotype. CHINA: Hainan Province, Ledong County, Hainan Tropical Rainforest National Park, Jianfengling National Natural Reserve, Mingfeng Valley, approximately 108°53′ E and 18°43′ N, elevation approximately 720 m, saprobic on dead corticated branches of *Cyclobalanopsis*, 23 October 2020, Haixia Ma, Col. J217 (FCATAS 2714).

Teleomorph. Stromata pulvinate to effused–pulvinate, 0.1–2 cm long × 0.1–0.6 cm broad × 0.25–0.45 mm thick; with inconspicuous perithecial mounds; surface Livid Purple (81), Livid Vinaceous (83) and Violet (32), with colored coating worn off exposing Dark Purple (36) areas, sometimes with tiny cracks appearing; with pale-brown to orange-brown granules immediately beneath the surface and between perithecia; yielding Amber (47) and Ochreous (44) to Fulvous (43) pigments in 10% KOH; tissue below the perithecial layer inconspicuous and pale-brown to black. Perithecia ovoid to obovoid, black, 0.1–0.3 mm broad × 0.1–0.4 mm high. Ostioles umbilicate, encircled with a white area, opening lower than the stromatal surface. Asci cylindrical, eight-spored, uniseriate, short-stipitate, 76–117 μm total length × 6.9–12.9 μm broad, the spore-bearing portion 65–93 μm long, and stipes 6–28 μm long, with apical apparatus highly reduced and minute, faintly bluing in Melzer's reagent. Ascospores brown to dark-brown, unicellular, ellipsoid-inequilateral, with narrowly to broadly rounded ends, 11–15.2 × 5.1–7 μm (n = 60, M = 13 × 6.3 μm), with more sigmoid to less straight spore-length germ slit on the convex side; perispore dehiscent in 10% KOH, with conspicuous coil-like ornamentation in SEM; epispore smooth.

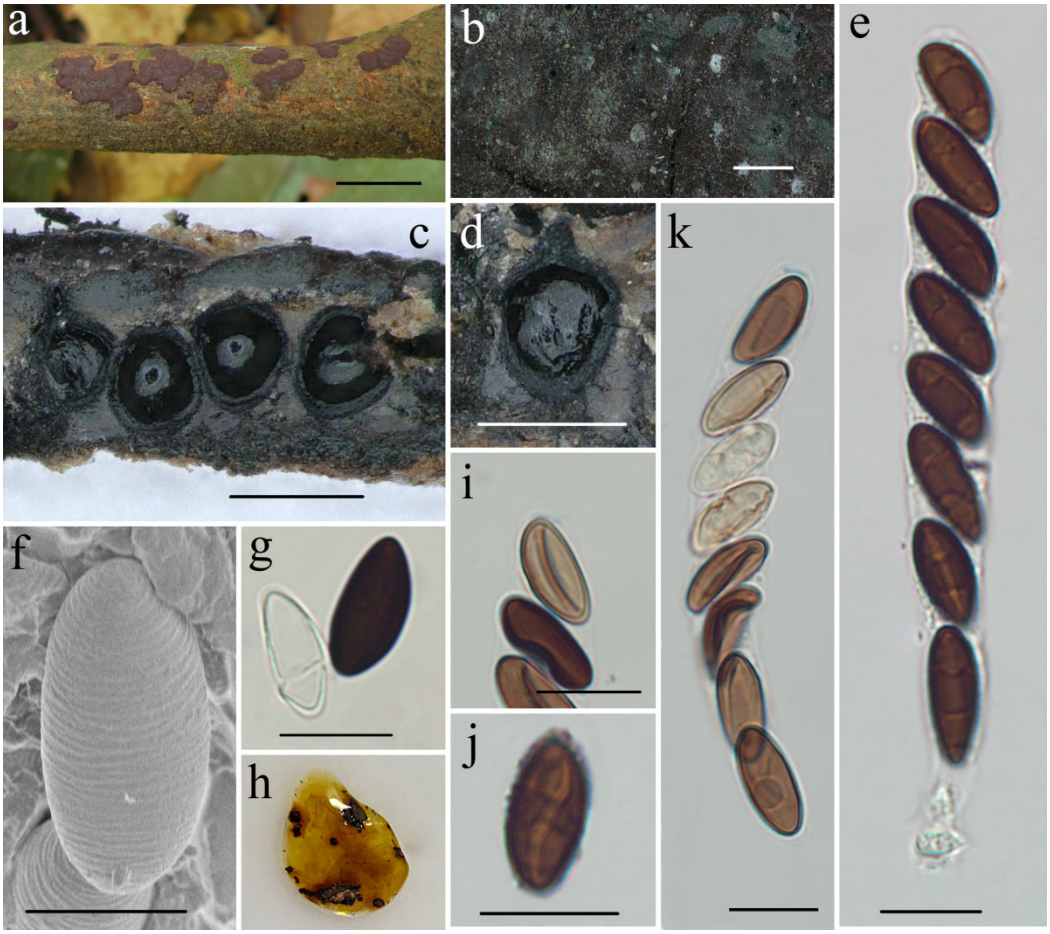

Figure 3. *Hypoxylon cyclobalanopsidis* (holotype FCATAS 2714). (**a**) Stromata on branches. (**b**) Stromatal surface and ostioles. (**c**,**d**) Stroma in vertical section showing the perithecia and tissue below the perithecial layer. (**e**) Mature ascus in water showing germ slit. (**f**) Ascospore under SEM. (**g**) Ascospore in 10% KOH. (**h**) KOH-extractable pigments. (**i**) Apical apparatus in Melzer's reagent. (**j**) Ascospore in water showing germ slit. (**k**) Ascus in Melzer's reagent. Scale bars: (**a**) = 1cm; (**b**–**d**) = 200 μm; (**e**,**g**,**i**–**k**) = 10 μm; (**f**) = 5 μm.

Additional specimens examined. CHINA: Hainan Province, Ledong County, Hainan Tropical Rainforest National Park, Jianfengling National Natural Reserve, Mingfeng Valley, approximately 108°51′ E and 18°45′ N, elevation approximately 700 m, saprobic on dead corticated branches of *Cyclobalanopsis*, 23 October 2020, Haixia Ma, Col. J200 (FCATAS 2715).

Hypoxylon hainanense Hai X. Ma, Z.K. Song, sp. nov., Figure 4.

MycoBank: MB 841955.

Diagnosis. Differs from *H. brevisporum* in having larger and wider ascospores, spherical to obovoid perithecia, and slightly larger apical apparatus. Differs from *H. lividicolor* in its thiner stromata, spherical to obovoid perithecia, and smaller ascospores.

Etymology. *Hainanense* (Lat.): referring to the holotype locality of species in Hainan Province.

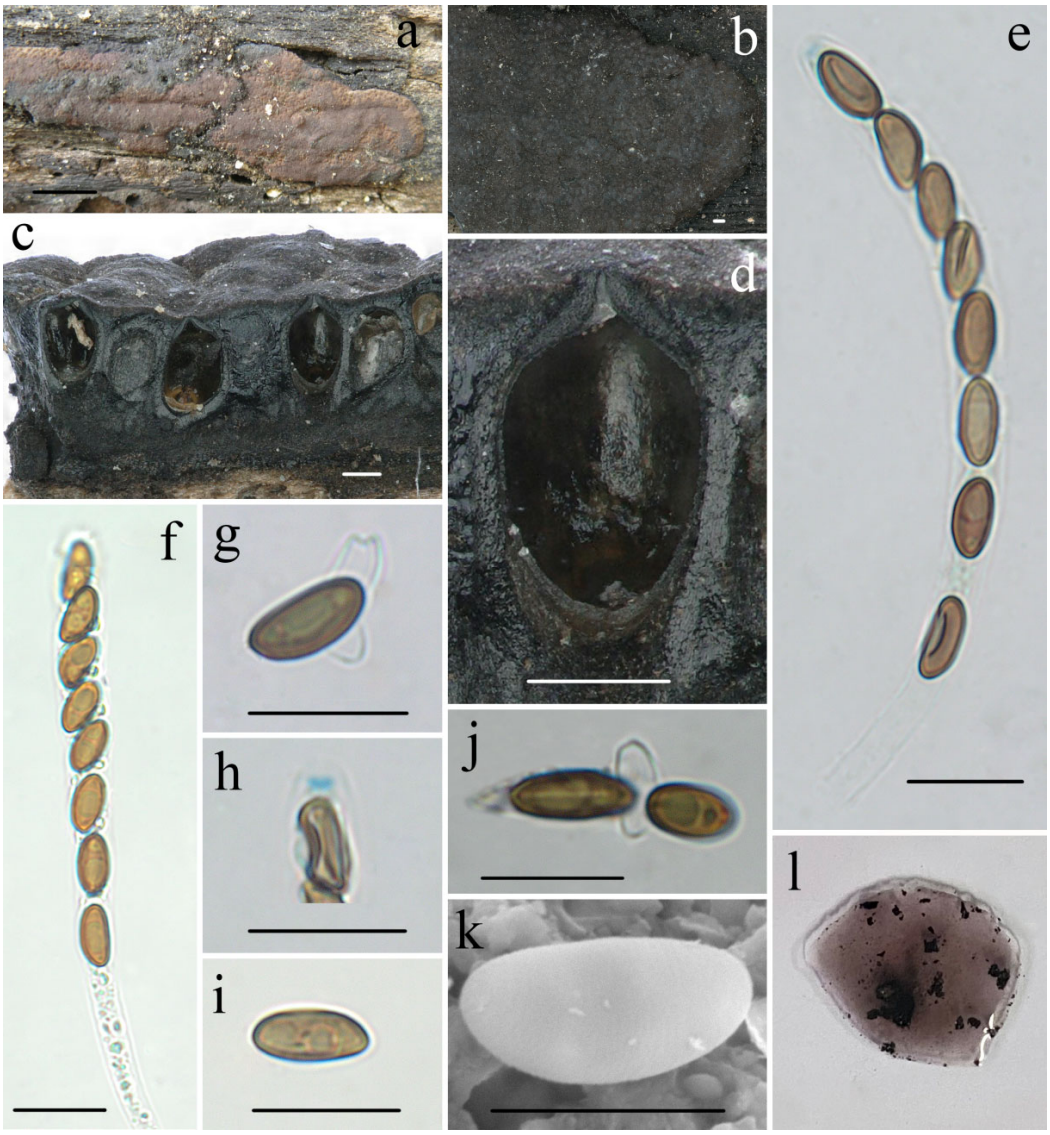

Figure 4. *Hypoxylon hainanense* (holotype FCATAS 2712). (**a**) Stromata on wood. (**b**) Stromatal surface. (**c**,**d**) Stroma in vertical section showing the perithecia and tissue below the perithecial layer. (**e**) Ascus in Melzer's reagent. (**f**) Ascus in water. (**g**) Ascospore in 10% KOH. (**h**) Apical apparatus in Melzer's reagent. (**i**) Ascospore in water. (**j**) Ascospore in 10% KOH showing germ slit. (**k**) Ascospore under SEM. (**l**) KOH-extractable pigments. Scale bars: (**a**) = 1cm; (**b**–**d**) = 200 μm; (**e**–**j**) = 10 μm; (**k**) = 5 μm.

Holotype. CHINA: Hainan Province, Ledong County, Hainan Tropical Rainforest National Park, Jianfengling National Natural Reserve, approximately 108°48′ E and 18°45′ N, elevation approximately 650 m, saprobic on surface of dead decorticated wood, 29 December 2020, Haixia Ma, Col. J233 (FCATAS 2712).

Teleomorph. Stromata effused–pulvinate, 0.8–7.2 cm long × 0.6–3.3 cm broad × 0.7–1.5 mm thick; with inconspicuous to conspicuous perithecial mounds; surface Violet (32), Livid Purple (81) and Dark Violet (33); highly carbonaceous black granules immdediately beneath surface and between perithecia; yielding Pale Vinaceous (85) to Livid Vinaceous (83) and Vinaceous Purple (101) pigments in 10% KOH; tissue below the perithecial layer black, conspicuous, 0.3–0.8 mm thick. Perithecia spherical to obovoid, black, 0.2–0.5 mm broad × 0.3–0.6 mm high, occasionally with pale-brown perithecial contents. Ostioles opening at the same level or slightly higher than the stromatal surface. Asci cylindrical, eight-spored, uniseriate, 70–139 μm total length × 4.6–6.8 μm broad, the spore-bearing portion 47–61 μm long, and stipes 19–83 μm long, with amyloid apical apparatus bluing in Melzer's reagent, discoid, 0.6–1.1 μm high × 1.3–1.8 μm broad. Ascospores light-brown

to brown, unicellular, ellipsoid-inequilateral, with slightly broad rounded ends, 6.1–9.6 × 3.2–5 μm (n = 60, M = 7.7 × 4 μm), with conspicuously straight germ slit less than spore-length on the convex side; perispore dehiscent in 10% KOH, with inconspicuous coil-like ornamentation in SEM; epispore smooth.

Additional specimens examined. CHINA: Hainan Province, Ledong County, Hainan Tropical Rainforest National Park, Jianfengling National Natural Reserve, approximately 108°50′ E and 18°46′ N, elevation approximately 600 m, saprobic on surface of dead decorticated wood, 29 December 2020, Haixia Ma, Col. J1058 (FCATAS 2713).

Hypoxylon wuzhishanense Hai X. Ma, Z.K. Song, sp. nov., Figure 5.

MycoBank: MB 841954.

Diagnosis. Differs from *H. pseudofendleri* by having smaller prithecia, larger ascospores and lower ostioles. Differs from *H. pilgerianum* in having larger apical apparatus, larger and wider ascospores, and most of perispore indehiscent in 10% KOH.

Etymology. *Wuzhishanense* (Lat.): referring to the holotype locality of species in Wuzhishan National Natural Reserve.

Holotype. CHINA: Hainan Province, Wuzhishan City, Hainan Tropical Rainforest National Park, Wuzhishan National Natural Reserve, approximately 109°38′ E and 18°55′ N, elevation approx. 600 m, saprobic on surface of dead *Bamboo* sp., 30 December 2020, Haixia Ma, Col. W2 (FCATAS 2708).

Teleomorph. Stromata pulvinate, 0.8–14 cm long × 0.4–3.2 cm broad × 0.2–0.3 mm thick; with inconspicuous-to-conspicuous perithecial mounds; surface Rust (39), Livid Purple (81) to Dark Brick (60), with colored coating worn off exposing Dark Purple (36) areas, with yellowish-brown granules immediately beneath the surface and between perithecia; yielding Amber (47) and Ochreous (44) to Fulvous (43) pigments in 10% KOH; tissue below the perithecial layer inconspicuous. Perithecia spherical, black, 0.2–0.3 mm broad × 0.1–0.2 mm high. Ostioles umbilicate, opening slightly lower than the stromatal surface. Asci cylindrical, eight-spored, uniseriate, 71–106 μm total length × 6.4–9 μm broad, the spore-bearing portion 58–91 μm long, and stipes 9–28 μm long, with amyloid apical apparatus bluing in Melzer's reagent, discoid, 1–1.9 μm high × 2.2–3.4 μm broad. Ascospores light-brown to brown, unicellular, ellipsoid-inequilateral, with narrowly rounded ends, (9.5–)10–14 × 5.4–6.7 μm (n = 60, M = 11.4 × 6 μm), with straight to less frequently sigmoid germ slit spore-length on the convex side; most of perispore indehiscent in 10% KOH, occasionally dehiscent, with inconspicuous coil-like ornamentation in SEM; epispore smooth.

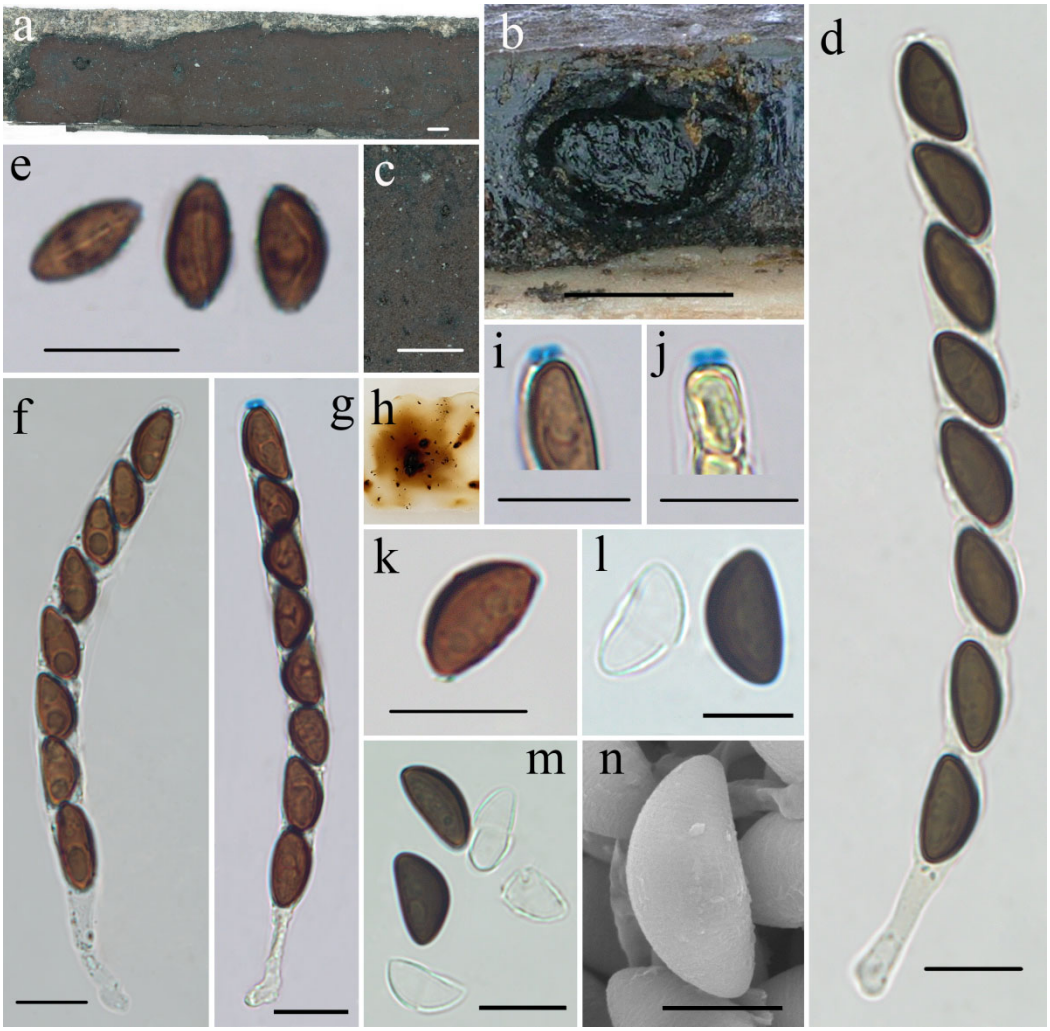

Figure 5. *Hypoxylon wuzhishanense* (holotype FCATAS 2708). (**a**) Stromata on dead *Bamboo* sp. (**b**) Stroma in vertical section showing the perithecia and tissue below the perithecial layer. (**c**) Stromatal surface and ostioles. (**d**) Ascus in 10% KOH. (**e**) Ascospores in Melzer's reagent showing germ slit. (**f**) Ascus in water. (**g**) Ascus in Melzer's reagent. (**h**) KOH-extractable pigments. (**i**,**j**) Apical apparatus in Melzer's reagent. (**k**) Ascospore in water. (**l**,**m**) Ascospore in 10% KOH. (**n**) Ascospore under SEM. Scale bars: (**a**) = 1 mm; (**b**,**c**) = 200 μm; (**d**–**g**,**i**–**m**) = 10 μm; (**g**) = 5 μm.

Additional specimens examined. CHINA: Hainan Province, Wuzhishan City, Hainan Tropical Rainforest National Park, Wuzhishan National Natural Reserve, approximately 109°38′ E and 18°55′ N, elevation approximately 600 m, saprobic on surface of dead *Bamboo* sp., 30 December 2020, Haixia Ma, Col. X469 (FCATAS 2709).

Key to *Hypoxylon* species from China and related species around the world

1. Ostioles barely to slightly higher than the stromatal surface 2
1. Ostioles lower than the stromatal surface 8
2. Ascospores nearly equilateral 3
2. Ascospores inequilateral 4
3. Stromata glomerate to pulvinate; ascospores 8.5–12(–13.5) × 4–5 μm ..... ***H. croceum***
3. Stromata pulvinate to effused–pulvinate; ascospores 11–14.5 × (4.5–)5–6.5 μm ..... ***H. parksianum***
4. Perithecia tubular..... 5
4. Perithecia subglobose, spherical to obovoid 6

5. Perithecia 0.5–0.85 mm broad × 0.35–0.5mm high ..... ***H. pseudofendleri***
5. Perithecia 0.2–0.3 mm broad × 0.4–0.6 mm high ..... ***H. lienhwacheense***
6. Ascospores light-brown to brown ..... ***H. hainanense***
6. Ascospores brown to dark-brown 7
7. Perithecia 0.3–0.5(–0.6) mm broad; ascospores 9.5–15(–16) × 4–6.5(–7) μm ..... ***H. lenormandii***
7. Perithecia 0.1–0.2 mm broad; ascospores 7.5–9.5 × 3.5–4.5 μm ..... ***H. rutilum***
8. Ascospores nearly equilateral 9
8. Ascospores inequilateral 14
9. Perispore dehiscent in 10% KOH ..... ***H. hypomiltum***
9. Perispore indehiscent in 10% KOH 10
10. KOH-extractable pigment Orange (7) ..... ***H. cinnabarinum***
10. Without apparent KOH-extractable pigments or with other colors 11
11. Without apparent KOH-extractable pigments or with dilute Grayish Sepia (106) to blackish pigments ..... ***H. dieckmannii***
11. KOH-extractable pigments greenish to olivaceous 12
12. Perithecia tubular to long tubular, 0.3–0.4 mm broad × 0.5–1 mm high .. ***H. investiens***
12. Perithecia spherical to obovoid, less than 0.3 mm broad 13
13. Stromatal surface Vinaceous Gray (116), Purplish Gray (128), Livid Vinaceous (83), Dark Vinaceous (82), or Brown Vinaceous (83), becoming blackish when aged; dull reddish-brown granules immediately beneath surface and between perithecia; asci with apical apparatus bluing in Melzer's reagent; ascospores dark-brown to blackish-brown, pyriform to obovoid, (11.5–)12–15(–16) × 5.5–7 μm ..... ***H. fuscopurpureum***
13. Stromatal surface Fawn (87) or Umber (9); blackish granules immediately beneath surface and between perithecia; asci with apical apparatus lightly bluing in Melzer's reagent; ascospores brown, ellipsoid, 7–8.5 × 4–4.5 μm .....……. ***H. gilbertsonii***
14. Sigmoid germ slit .....…… 15
14. Straight or slightly sigmoid germ slit 17
15. Stromata glomerate, with conspicuous perithecial mounds; KOH-extractable pigments Pure Yellow (14) with Citrine (13) tone, Greenish Olivaceous (90), or Orange (7) ..... ***H. musceum***
15. Stromata pulvinate or effused–pulvinate, with inconspicuous to conspicuous perithecial mounds; KOH-extractable pigments with other colors 16
16. Asci with apical apparatus bluing in Melzer's reagent, 0.5–1.2 μm high × 1.8–2.5 μm broad; KOH-extractable pigment Orange (7) .....…..... ***H. fendleri***
16. Asci with apical apparatus bluing in Melzer's reagent, 0.5–0.8 μm high × 3–3.4 μm broad; KOH-extractable pigment Vinaceous Purple (101) .....…..... ***H. fuscoides***
17. Straight germ slit …..... 18
17. Straight or slightly sigmoid germ slit 26
18. Straight germ slit slightly less than spore length; perispore infrequently dehiscent in 10% KOH ..... ***H. dengii***

18. Straight spore-length germ slit; perispore dehiscent in 10% KOH 19
19. Perithecia long tubular …..... 20
19. Perithecia spherical to obovoid …..... 21
20. Stromatal surface Fulvous (43), Sienna (8), or Rust (39); stromata containing orange-red granules, with KOH-extractable pigments Orange (7) or Scarlet (5); asci with apical apparatus bluing in Melzer's reagent, 1–2(–2.5) μm high × 3–4 μm broad ..... ***H. haematostroma***
20. Stromatal surface Brown Vinaceous (84), Dark Brick (60), Sepia (63), or Chestnut (40); stromata containing dark-reddish-brown or blackish granules, with KOH-extractable pigments Olivaceous (48), Greenish Olivaceous (90), Isabelline (65), or Dull Green (70), or infrequently without apparent pigments; asci with apical apparatus bluing in Melzer's reagent, 0.5–1 μm high × 2.5–3 μm broad ..... ***H. placentiforme***
21. KOH-extractable pigments Olivaceous Gray (12), Greenish Olivaceous (90), or Gray Olivaceous (107) ..... ***H. brevisporum***
21. KOH-extractable pigments with other colors 22
22. Conspicuous coil-like ornamentation of perispore; asci with apical apparatus not bluing in Melzer's reagent 23
22. Smooth or with inconspicuous coil-like ornamentation of perispore; asci with apical apparatus bluing to lightly bluing in Melzer's reagent 24
23. KOH-extractable pigments Orange (7), Sienna (8), and Amber (47). ***H. baihualingense***
23. KOH-extractable pigments Pale Luteous (11), Citrine (13) and Honey (64) ..... ***H. chrysalidosporum***
24. Stromata on bamboo ..... ***H. pilgerianum***
24. Stromata on dicot wood 25
25. Stromata effused–pulvinate, plane, or with inconspicuous to conspicuous perithecial mounds; perithecia 0.2–0.5 mm broad × 0.3–0.6 mm high; smooth or with inconspicuous coil-like ornamentation of perispore ..... ***H. rubiginosum***
25. Stromata pulvinate with conspicuous perithecial mounds; perithecia 0.1–0.2 mm broad × 0.2–0.3 mm high; smooth perispore ..... ***H. vinosopulvinatum***
26. Perithecia 0.5–0.7 mm broad ..... ***H. wujiangensis***
26. Perithecia less than 0.3 mm broad 27
27. Perispore indehiscent in 10% KOH ..... ***H. wuzhishanense***
27. Perispore dehiscent in 10% KOH 28
28. Conspicuous coil-like ornamentation of perispore 29
28. Smooth or with inconspicuous coil-like ornamentation of perispore 32
29. Stromata glomerate to hemispherical 30
29. Stromata pulvinate to effused–pulvinate 31
30. Stromata glomerate, restricted-pulvinate to effused–pulvinate, 0.1–6 cm long × 0.1–1.5 cm broad; asci with apparatus bluing in Melzer's reagent; ascospores with straight or slightly sigmoid spore-length germ slit ..... ***H. duranii***

30. Stromata hemispherical, pulvinate to effused–pulvinate, up to 12 cm long × 0.2–2 cm broad; asci with apical apparatus bluing in Melzer's reagent; ascospores with more sigmoid or less straight spore-lenth germ slit ..... ***H. eurasiaticum***
31. Asci with apical apparatus highly reduced, minute, faintly bluing in Melzer's reagent; ascospores 11–15.2 × 5.1–7 μm, with more sigmoid or less straight spore-length germ slit ..... ***H. cyclobalanopsidis***
31. Asci with apical apparatus bluing in Melzer's reagent, 0.5–1 μm high × 2–2.5 μm broad; ascospores (9–)9.5–12 × 4.5–5 μm, with straight or slightly sigmoid spore-length germ slit ..... ***H. retpela***
32. Stromata hemispherical to spherical 33
32. Stromata pulvinate to effused–pulvinate 36
33. KOH-extractable pigments Orange (7) or Rust (39) ..... ***H. howeanum***
33. KOH-extractable pigments with other colors 34
34. Asci with apical apparatus highly reduced or lacking, not bluing in Melzer's reagent; ascospores (11–)12–16 × (5.5–)6–7.5 μm ..... ***H. notatum***
34. Asci with apical apparatus bluing in Melzer's reagent 35
35. Perithecia spherical to obovoid, 0.1–0.3(–0.4) mm broad × 0.2–0.5 mm high; ascospores 8-20 × 4-8 μm, with slightly sigmoid germ slit ..... ***H. fuscum***
35. Perithecia spherical, 0.1-0.3 mm diameter; ascospores (8–)9–12(–13) × 4–6 μm, with straight or slightly sigmoid germ slit ..... ***H. perforatum***
36. Ascospore length less than 11 μm 37
36. Ascospore length more than 11 μm 39
37. KOH-extractable pigments Pure Yellow (14) or Amber (47) ..... ***H. trugodes***
37. KOH-extractable pigment Orange (7) 38
38. Stromatal surface Fulvous (43), Ochreous (44), or Apricot (42); asci with apical apparatus 0.2–0.5 μm high × 1–1.5 μm broad; ascospores 8–9.5(–11) × 4–5 μm; *Periconiella*-like conidiogenous structure ..... ***H. jecorinum***
38. Stromatal surface Umber (9), Sepia (63), Rust (39), Sienna (8), Dark Brick (60), or Bay (6); asci with apical apparatus 0.3–1 μm high × 1.5–2.2 μm broad; ascospores 7–11 × 3.5–5 μm; *Nodulisporium*-like conidiogenous structure ..... ***H. subgilvum***
39. KOH-extractable pigment Orange (7) ..... ***H. crocopeplum***
39. KOH-extractable pigments with other colors 40
40. KOH-extractable pigment Dark Livid (80) 41
40. KOH-extractable pigments greenish to olivaceous 42
41. Stromata 2.5 mm thick; ascospores 11–12.5 × 4.5–5 μm ..... ***H. lividicolor***
41. Stromata 0.8–1 mm thick; ascospores 10–13.5(–15) × 4.5–6 μm ..... ***H. lividipigmentum***
42. Perithecia obovoid to tubular ..... ***H. anthochroum***
42. Perithecia spherical to obovoid 43
43. Perithecia 0.18–0.35 mm broad × 0.28–0.42 mm high; ascospores (9–)10–13.5 × 4–5 μm ..... ***H. porphyreum***
44. Perithecia 0.12–0.28 mm broad × 0.19–0.36mm high; ascospores 11–16 × 4.5–7.3 μm ..... ***H. pseudofuscum***

4. Discussion

Hainan Tropical Rainforest National Park is primarily tropical lowland and tropical mountain rainforest, enjoying a tropical island monsoon climate moderated by a hot and moist climate with annual rainfall often over 2200 mm (http://www.hntrnp.com, accessed on 15 November 2021). The pattern raises the high diversity and the high number of endemic species of vegetation and fungi in the region. *Hypoxylon* is a cosmopolitan genus, but in tropical and subtropical regions it displays a higher diversity [4]. In the present study, four new species of *Hypoxylon* from Hainan Tropical Rainforest National Park are described, based on morphological characteristics and phylogenetic analyses of the ITS, LSU, RPB2, and β-tubulin sequences. The secondary metabolite profiles generated from chemotaxonomic studies provide strong support for identifying species. However, chemotaxonomic data were not generated in this study [3].

Phylogenetically, *H. chrysalidosporum* is closely related to *H. duranii* J. D. Rogers, based on a combined ITS–LSU–RPB2–β-tubulin dataset. *Hypoxylon duranii* was originally described from Mexico, but the holotype lacked phylogenetic data. Sequence data for *H. duranii* collected from China were referenced in this study [4,16]. Morphologically, *H. duranii* is similar to *H. chrysalidosporum*, sharing glomerate and effused–pulvinate stromata, spherical to obovoid perithecia, and dehiscent perispore with conspicuous coil-like ornamentation. However, *H. duranii* can be distinguished from *H. chrysalidosporum* by its KOH-extractable pigments Isabelline or Amber, amyloid apical apparatus, bluing in Melzer's reagent, and slighly larger ascospores [9.5–13(–14.5) × 4.5–6.5 μm] with a straight or slightly sigmoid germ slit [4]. *Hypoxylon chrysalidosporum* resembles *H. notatum* Berk., M. A. Curtis apud Berk. and *H. shearii* Y.-M. Ju, J. D. Rogers in having a similar stromatal morphology, apical apparatus being highly reduced or absent, not bluing in Melzer's reagent, and having dehiscent perispore [4]. However, the type of *H. notatum* was selected by Miller (1961) from the southern United States, and differs in having KOH-extractable pigments Pure Yellow with Greenish Yellow tone and Dark Brown, and larger ascospores [(11–)12–16 × (5.5–)6–7.5 μm] which are strongly curved [1,4]. *H. shearii* has a buff or fawn stromatal surface, with Luteous KOH-extractable pigments, larger prithecia (0.4–0.7 mm diameter), and dark-brown, larger ascospores [12–14 × 5.5–6.5(–7) μm] [4].

Hypoxylon cyclobalanopsidis is closely related to *H. porphyreum* Granmo, *H. eurasiaticum* Pourmoghaddam, Krisai-Greilhuber, Khodap., *H. fuscum* (Pers.: Fr.) Fr., and *H. pseudofuscum* Pourmoghaddam, Khodap., Krisai-Greilhuber in the phylogenetic analyses (Figure 1). *Hypoxylon porphyreum* differs from *H. cyclobalanopsidis* in its smaller ascospores [(9–)10–13.5 × 4–5 μm, M = 11.4 × 4.8 μm], KOH-extractable pigments Brown with a Greenish tone, and growing on *Quercus* from southeastern Norway, Sweden, France and the USA [60,61]. *Hypoxylon eurasiaticum* can be distinguished from *H. cyclobalanopsidis* by its larger discoid apical apparatus (0.5–1.5 μm high × 2.5–3.5 μm wide), smaller ascospores (9–12.5 × 4–6 μm), and by growing on *Quercus castaneifolia* from Iran [33]. *Hypoxylon fuscum* is primarily distinguished from *H. cyclobalanopsidis* by its hemispherical to pulvinate stromata with dull orange, dull orange-brown, or dull reddish-brown granules immediately beneath the surface and between perithecia, larger discoid apical apparatus (0.5–2 μm high × 1.2–3.5 μm wide), slightly larger ascospores (12.5–15.5 × 5–7 μm), and it frequently occurs on *Corylus avellana* in Europe [4,62,63]. *Hypoxylon pseudofuscum* has larger discoid apical apparatus (0.5–1.5 μm high × 2–3.5 μm wide), KOH-extractable pigments Isabelline,or Hazel, slightly larger ascospores (11–16 × 4.5–7.3 μm), and it grows on *Alnus* and *Salix* from Germany and Iran [33].

Hypoxylon hainanense is closely related to *H. brevisporum* Y.M. Ju, J.D. Rogers, *H. lividipigmentum* F. San Martín, Y.M. Ju, J.D. Rogers, and *H. lividicolor* Y.-M. Ju, J. D. Rogers, with a weak bootstrap value according to ML phylogenetic analyses (Figure 1). *Hypoxylon brevisporum* differs from *H. hainanense* in having KOH-extractable pigment Olivaceous Gray, obovoid to tubular perithecia, smaller and thiner ascospores (5.5–8 × 2.5–3.5 μm), and slightly smaller apical apparatus (0.2–0.4 μm high × 1.2–1.5 μm broad) [4]. *Hypoxylon lividicolor* is distinguished by its thicker, chestnut stromata with KOH-extractable pigment

Dark Livid, tubular to long tubular perithecia, and larger dark-brown ascospores (11–12.5 × 4.5–5 μm) with straight or slightly sigmoid germ slit [4]. *Hypoxylon lividipigmentum* differs in having tubular to long tubular perithecia and larger, dark-brown ascospores [10–13.5(–15) × 4.5–6 μm] [4].

Hypoxylon wuzhishanense is closely related to *H. pseudofendleri* D.Q. Dai, K.D. Hyde in our phylogenetic analyses (Figure 1). Unfortunately, RPB2 and β-tubulin sequences of *H. pseudofendleri* are not available for phylogenetic analysis in GenBank. Morphologically, *H. pseudofendleri* is similar to *H. wuzhishanense* in having large, purplish-brown stromata, yellowish-brown granules beneath the surface and between perithecia, similar asci and apical apparatus. However, *H. pseudofendleri* differs from *H. wuzhishanense* in having larger perithecia (500–850 μm broad × 350–500 μm high), with ostioles slightly higher than the stromatal surface, and slightly smaller ascospores (9–11.5 × 4.5–6.5 μm, M = 10.2 × 5.7 μm) with slighly pointed at the ends and smooth wall [42]. There are no descriptions of stromatal pigments in 10% KOH, germination site of ascospores, or perispore in 10% KOH for *H. pseudofendleri*, so we cannot compare these characteristics between the two species. The two species group together with *H. pilgerianum* Henn. *Hypoxylon pilgerianum* was originally described from Brazil on *Chusquea* sp., with ascospores 10–12 × 4–5 μm (M = 11 × 4.5 μm), and reinstated by Ju and Rogers on dead culms of bamboo, with ascospores 8.5–12(–13.5) × 4–5(–5.5) μm (M = 10.3 × 4.5 μm) [4,9,64]. Fournier et al. described two collections from Martinique as *H.* cf. *pilgerianum* sp. 1 and *H.* cf. *pilgerianum* sp. 2, with ascospores (7.6–)7.9–9.1(–10) × (3.4–)3.7–4.3(–4.4) μm (M = 8.5 × 4 μm) and (10.3–)10.9–12.5(–12.8) × (4.9–)5.2–6.1(–6.7) μm (M = 11.6 × 5.7 μm), respectively [9]. *Hypoxylon pilgerianum* s. Ju, Rogers resembles *H. wuzhishanense* in stromatal morphology, but the former has slighly smaller apical apparatus (0.5–1 μm high × 2.5 μm broad), and smaller and thinner ascospores [8.5–12(–13.5) × 4–5(–5.5) μm], with perispore dehiscent in 10% KOH [4]. *Hypoxylon fuscopurpureum* (Schwein.) M. A. Curtis somewhat resembles *H. wuzhishanense*, sharing its stromatal morphology, but differs in having greenish KOH-extractable pigments and larger asci (115–150 × 8–10 μm) [4].

Most species of *Hypoxylon* play an important ecological role in tropical rainforests as wood-decomposers [3], and some might have benefical effects on their hosts during their endophytic life stage [65]. In addition, many species have been found to produce highly bioactive secondary metabolites [41,43,66–70]. Although approximately 33 species of *Hypoxylon* have been recorded in China [4,19–21,29,71], species diversity, evolution, population dynamics, and the host–fungus interactions of this genus are still obscure. Therefore, comprehensive studies on the diversity, phylogeny, evolution, host–fungus interactions, and secondary metabolites of the genus *Hypoxylon* are needed in the future.

5. Conclusions

The current study revealed four new taxa of *Hypoxylon* from Hainan Tropical Rainforest National Park based on morphological characteristics, ecological distributions, and a combined ITS–LSU–RPB2–β-tubulin phylogeny.

Author Contributions: H.M. designed the research; H.M., Z.S., X.P., Z.Y., and Z.Q. prepared the samples; Z.S. conducted the molecular experiments and analyzed the data; Z.S. and H.M. drafted the manuscript; Y.L. revised the language of the text. All authors have read and agreed to the published version of the manuscript.

Funding: The research was supported by the National Natural Science Foundation of China (No. 31972848, 31770023), Key Research and Development Program of Hainan (ZDYF2020062), and Hainan Basic and Applied Research Project for Cultivating High-Level Talents (2019RC305).

Institutional Review Board Statement: Not applicable.

Data Availability Statement: Publicly available datasets were analyzed in this study. All resulting alignments were deposited in TreeBASE (http://www.treebase.org; accession number S29126). All newly generated sequences were deposited in GenBank (https://www.ncbi.nlm.nih.gov/genbank/;

Table 1). All new taxa were deposited in MycoBank (https://www.mycobank.org/; MycoBank identifiers follow new taxa).

Acknowledgments: We express our gratitude to Shuang-hui He (Beijing Forestry University, China) for help during field collections. Hainan Tropical Rainforest National Park Service is thanked for providing collecting facilities in Jianfengling and Wuzhishan National Natural Reserve.

Conflicts of Interest: The authors declare no conflict of interest. The funders had no role in the design of the study; in the collection, analyses, or interpretation of data; in the writing of the manuscript, or in the decision to publish the results.

References

1. Miller, J.H. *A Monograph of the World Species of Hypoxylon*; University Georgia Press: Athens, Greece, 1961; p. 158.
2. Rogers, J.D. The Xylariaceae: systematic, biological and evolutionary aspects. *Mycologia* **1979**, *71*, 1–42.
3. Stadler, M. Importance of secondary metabolites in the Xylariaceae as parameters for assessment of their taxonomy, phylogeny, and functional biodiversity. *Curr. Res. Envion. Appl. Mycol.* **2011**, *1*, 75–133.
4. Ju, Y.M.; Rogers, J.D. *A revision of the Genus Hypoxylon*; American Phytopathological Society Press: St. Paul, MN, USA, 1996; p. 365.
5. Rogers, J.D. Thoughts and musings on tropical Xylariaceae. *Mycol. Res.* **2000**, *104*, 1412–1420.
6. Kuhnert, E.; Fournier, J.; Per, D.; Luangsaard, J.J.D.; Stadler, M. New *Hypoxylon* species from Martinique and new evidence on the molecular phylogeny of *Hypoxylon* based on ITS rDNA and β-tubulin data. *Fungal Divers.* **2014**, *64*, 181–203.
7. Hyde, K.D.; Norphanphoun, C.; Maharachchikumbura, S.S.N.; Bhat, D.J.; Jones, E.B.G.; Bundhun, D. Refined families of Sordariomycetes. *Mycosphere* **2020**, *11*, 305–1059. https://doi.org/10.5943/mycosphere/11/1/7.
8. Pourmoghaddam, M.J.; Lambert, C.; Surup, F.; Khodaparast, S.A.; Krisai-Greilhuber, I.; Voglmayr, H.; Stadler, M. Discovery of a new species of the *Hypoxylon rubiginosum* complex from Iran and antagonistic activities of *Hypoxylon* spp. Against the Ash Dieback pathogen, *Hymenoscyphus fraxineus*, in dual culture. *MycoKeys* **2020**, *66*, 105–133.
9. Fournier, J.; Lechat, C.; Courtecuisse, R. The genus *Hypoxylon* (Xylariaceae) in Guadeloupe and Martinique (French West Indies). *Ascomycete.org* **2016**, *7*, 145–212.
10. Sir, E.B.; Kuhnert, E.; Lambert, C.; Hladki, A.I.; Romero, A.I.; Stadler, M. New species and reports of *Hypoxylon* from Argentina recognized by a polyphasic approach. *Mycol. Prog.* **2016**, *15*, 42.
11. Rogers, J.D. Two new *Hypoxylon* species from Gabon. *Can. J. Bot.* **1981**, *59*, 1363–1364.
12. Rogers, J.D.; Candoussau, F. A new variety of *Hypoxylon cohaerens* from France. *Mycologia* **1980**, *72*, 826–829.
13. Rogers, J.D. *Hypoxylon weldeni*i var. *microsporum* and *H. punctidiscum*. *Mycologia* **1980**, *72*, 829–832.
14. Rogers, J.D.; Ju, Y.M.; Hemmes, D.E. *Hypoxylon rectangulosporum* sp. nov., *Xylaria psidii* sp. nov., and comments on taxa of *Podosordaria* and *Stromatoneurospora*. *Mycologia* **1992**, *84*, 166–172.
15. Gucht, K.V.; Ju, Y.M.; Rogers, J.D. New *Hypoxylon* species from Papua New Guinea and notes on some other taxa. *Mycologia* **1997**, *89*, 503–511.
16. Hsieh, H.; Ju, Y.M.; Rogers, J.D. Molecular phylogeny of *Hypoxylon* and closely related genera. *Mycologia* **2005**, *97*, 844–865.
17. Lambert, C.; Wendt, L.; Hladki, A.I.; Stadler, M.; Sir, E.B. *Hypomontagnella* (Hypoxylaceae): A new genus segregated from *Hypoxylon* by a polyphasic taxonomic approach. *Mycol. Prog.* **2019**, *18*, 187–201.
18. Wendt, L.; Sir, E.B.; Kuhnert, E.; Heitkämper, S.; Lambert, C.; Hladki, A.I.; Romero, A.I.; Luangsaard, J.J.; Srikitikulchai, P.; Per, D.; et al. Resurrection and emendation of the Hypoxylaceae, recognised from a multigene phylogeny of the Xylariales. *Mycol. Prog.* **2018**, *17*, 115–154.
19. Teng, S.C. *Fungi of China;* Science Press: Beijing, China, 1963; pp. 182–191.
20. Tai, F.L. *Sylloge Fungorum Sinicorum*; Science Press: Beijing, China, 1979; pp. 163–167.
21. Ma, H.X. Taxonomy and Molecular Phylogeny of Several Genera of Xylariaceae from China. Ph.D. Thesis, Jilin Agricultural University, Changchun, China, June 2011.
22. Chi, S.Q.; Xu, J.; Lu, B.S. Three New Chinese Records of *Hypoxylon*. *J. Fungal Res*. **2016**, *14*, 218–221.
23. Rayner, R.W. *A Mycological Colour Chart*; Commonwealth Mycological Institute: London, UK, 1970.
24. Gardes, M.; Bruns, T.D. ITS primers with enhanced specificity for basidiomycetes-application to the identification of mycorrhizae and rusts. *Mol. Ecol.* **1993**, *2*, 113–118.
25. O'donnell, K.; Cigelnik, E. Two divergent intragenomic rDNA ITS2 types within a monophyletic lineage of the fungus *Fusarium* are nonorthologous. *Mol. Phylogenet. Evol.* **1997**, *7*, 103–116.
26. White, T.J.; Bruns, T.D.; Lee, S.; Taylor, J.W. *Amplification and Direct Sequencing of Fungal Ribosomal RNA Genes for Phylogenetics—Science Direct*; Academic Press: San Diego, CA, USA, 1990; pp. 315–322.
27. Vilgalys, R.; Hester, M. Rapid genetic identification and mapping of enzymatically amplified ribosomal DNA from several *Cryptococcus* species. *J. Bacteriol.* **1990**, *172*, 4238–4246.
28. Liu, Y.J.; Whelen, S.; Hall, B.D. Phylogenetic relationships among ascomycetes: Evidence from an RNA polymerse II subunit. *Mol. Biol. Evol.* **1999**, *16*, 1799–1808.

29. Ma, H.X.; Qiu, J.Z.; Xu, B.; Li, Y. Two *Hypoxylon* species from Yunnan Province based on morphological and molecular characters. *Phytotaxa* **2018**, *376*, 027–036.
30. Kuhnert, E.; Sir, E.B.; Lambert, C.; Hyde, K.D.; Hladki, A.I.; Romero, A.I.; Rohde, M.; Stadler, M. Phylogenetic and chemotaxonomic resolution of the genus *Annulohypoxylon* (Xylariaceae) including four new species. *Fungal Divers.* **2017**, *85*, 1–43.
31. Stadler, M.; Læssøe, T.; Fournier, J.; Decock, C.; Schmieschek, B.; Tichy, H.V.; Peršoh, D. A polyphasic taxonomy of *Daldinia* (Xylariaceae). *Stud. Mycol.* **2014**, *77*, 1–143.
32. Vicente, T.F.L.; Goncalves, M.F.M.; Brandao, C.; Fidalgo, C.; Alves, A. Diversity of fungi associated with macroalgae from an estuarine environment and description of *Cladosporium rubrum* sp. nov. and *Hypoxylon aveirense* sp. nov. *Int. J. Syst. Evol. Microbiol.* **2021**, *71*, 004630.
33. Lambert, C.; Pourmoghaddam, M.J.; Cedeño-Sanchez, M.; Surup, F.; Khodaparast, S.A.; Krisai-Greilhuber, I.; Voglmayr, H.; Stradal, T.E.B.; Stadler, M. Resolution of the *Hypoxylon fuscum* complex (Hypoxylaceae, Xylariales) and discovery and biological characterization of two of its prominent secondary metabolites. *J. Fungi* **2021**, *7*, 131.
34. Sir, E.B.; Becker, K.; Lambert, C.; Bills, G.F.; Kuhnert, E. Observations on Texas hypoxylons, including two new *Hypoxylon* species and widespread environmental isolates of the *H. croceum* complex identified by a polyphasic approach. *Mycologia* **2019**, *11*, 832–856.
35. Friebes, G.; Wendelin, I. Studies on *Hypoxylon ferrugineum* (Xylariaceae), a rarely reported species collected in the urban area of Graz (Austria). *Ascomycete.org* **2016**, *8*, 83–90. https://doi.org/10.25664/art-0175.
36. Daranagama, D.A.; Camporesi, E.; Tian, Q.; Liu, X.Z.; Chamyuang, S.; Stadler, M.; Hyde, K.D. *Anthostomella* is polyphyletic comprising several genera in Xylariaceae. *Fungal Divers.* **2015**, *73*, 203–238.
37. Sir, E.B.; Kuhnert, E.; Surup, F.; Hyde, K.D.; Stadler, M. Discovery of new mitorubrin derivatives from *Hypoxylon fulvosulphureum* sp. nov. (Ascomycota, Xylariales). *Mycol. Prog.* **2015**, *14*, 28.
38. Vu, D.; Groenewald, M.; Vries, M.; Gehrmann, T.; Stielow, B.; Eberhardt, U.; Al-Hatmi, A.; Groenewald, J.Z.; Cardinali, G.; Houbraken, J.; et al. Large-scale generation and analysis of filamentous fungal DNA barcodes boosts coverage for kingdom fungi and reveals thresholds for fungal species and higher taxon delimitation. *Stud. Mycol.* **2019**, *92*, 135–154.
39. Bitzer, J.; Læssøe, T.; Fournier, J.; Kummer, V.; Decock, C.; Tichy, H.V.; Piepenbring, M.; Peršoh, D.; Stadler, M. Affinities of *Phylacia* and the daldinoid Xylariaceae, inferred from chemotypes of cultures and ribosomal DNA sequences. *Mycol. Res.* **2008**, *112*, 251–270.
40. Becker, K.; Lambert, C.; Wieschhaus, J.; Stadler, M. Phylogenetic assignment of the fungicolous *Hypoxylon invadens* (Ascomycota, Xylariales) and investigation of its secondary metabolites. *Microorganisms* **2020**, *8*, 1–14.
41. Kuhnert, E.; Surup, F.; Sir, E.B.; Lambert, C.; Hyde, K.D.; Hladki, A.I.; Romero, A.I.; Stadler, M. Lenormandins A—G, new azaphilones from *Hypoxylon lenormandii* and *Hypoxylon jaklitschii* sp. nov., recognised by chemotaxonomic data. *Fungal Divers.* **2015**, *71*, 165–184.
42. Dai, D.Q.; Phookamsak, R.; Wijayawardene, N.N.; Li, W.J.; Bhat, D.J.; Xu, J.C.; Taylor, J.E.; Hyde, K.D.; Chukeatirote, E. Bambusicolous fungi. *Fungal Divers.* **2017**, *82*, 1–105.
43. Bills, G.F.; González-Menéndez, V.; Martín, J.; Platas, G.; Fournier, J.; Peršoh, D.; Stadler, M. *Hypoxylon pulicicidum* sp. nov. (Ascomycota, Xylariales), a pantropical insecticide-producing endophyte. *PLoS ONE* **2012**, *7*, e46687.
44. Stadler, M.; Kuhnert, E.; Peršoh, D.; Fournier, J. The Xylariaceae as model example for a unified nomenclature following the "One Fungus-One Name" (1F1N) concept. *Mycology* **2013**, *4*, 5–21.
45. Cedeño-Sanchez, M.; Wendt, L.; Stadler, M.; Mejía, L.C. Three new species of *Hypoxylon* and new records of Xylariales from Panama. *Mycosphere* **2020**, *11*, 1457–1476.
46. Phookamsak, R.; Hyde, K.D.; Jeewon, R.; Bhat, D.J.; Jones, E.B.G.; Maharachchikumbura, S.S.; Raspe, O.; Karunarathna, S.C.; Wanasinghe, D.N.; Hongsanan, S..; et al. Fungal diversity notes 929–1035: taxonomic and phylogenetic contributions on genera and species of fungi. *Fungal Divers.* **2019**, *95*, 1–273.
47. Stadler, M.; Fournier, J.; Laessøe, T.; Chlebicki, A.; Lechat, C.; Flessa, F.; Rambold, G.; Peršoh, D. Chemotaxonomic and phylogenetic studies of *Thamnomyces* (Xylariaceae). *Mycoscience* **2010**, *51*, 189–207.
48. Katoh, K.; Rozewicki, J.; Yamada, K.D. MAFFT online service: Multiple sequence alignment, interactive sequence choice and visualization. *Brief. Bioinform.* **2019**, *20*, 1160–1166.
49. Felsenstein, J. Evolutionary trees from DNA sequences: A maximum likelihood approach. *J. Mol. Evol.* **1981**, *17*, 368–376.
50. Tamura, K.; Peterson, D.; Peterson, N.; Stecher, G.; Nei, M.; Kumar, S. MEGA5: Molecular evolutionary genetics analysis using maximum likelihood, evolutionary distance, and maximum parsimony methods. *Mol. Biol. Evol.* **2011**, *28*, 2731–2739.
51. Stamatakis, A. Raxml version 8: a tool for phylogenetic analysis and post-analysis of large phylogenies. *Bioinformatics* **2014**, *9*, 1312–1313.
52. Darriba, D.; Taboada, G.L.; Doallo, R.; Posada, D. jModelTest 2: more models, new heuristics and parallel computing. *Nat. Methods* **2012**, *9*, 772.
53. Rannala, B.; Yang, Z. Probability distribution of molecular evolutionary trees: a new method of phylogenetic inference. *J. Mol. Evol.* **1996**, *43*, 304–311.
54. Huelsenbeck, J.P.; Ronquist, F. MRBAYES: Bayesian inference of phylogenetic trees. *Bioinformatics* **2001**, *17*, 754–755.
55. Hsieh, H.; Lin, C.; Fang, M.; Rogers, J.D.; Fournier, J.; Lechat, C.; Ju, Y.M. Phylogenetic status of *Xylaria* subgenus *Pseudoxylaria* among taxa of the subfamily Xylarioideae (Xylariaceae) and phylogeny of the taxa involved in the subfamily. *Mol. Phylogenet. Evol.* **2010**, *54*, 957–969.

56. Ronquist, F.; Teslenko, M.; Mark, P.; Ayres, D.L.; Darling, A.; Höhna, S.; Larget, B.; Liu, L.; Suchard, M.A.; Huelsenbeck, J.P. Mrbayes 3.2: Efficient bayesian phylogenetic inference and model choice across a large model space. *Syst. Biol.* **2012**, *61*, 539–542.
57. Daranagama, D.A.; Hyde, K.D.; Sir, E.B.; Thambugala, K.M.; Stadler, M. Towards a natural classification and backbone tree for Graphostromataceae, Hypoxylaceae, Lopadostomataceae and Xylariaceae. *Fungal Divers.* **2018**, *88*, 1–165.
58. Long, Q.D.; Liu, L.L.; Zhang, X.; Wen, T.C.; Kang, J.C.; Hyde, K.D.; Shen, X.C.; Li, Q.R. Contributions to species of Xylariales in China-1. *Durotheca* species. *Mycol. Prog.* **2019**, *18*, 495–510.
59. Rambaut, A. Figtree Version 1.4.2. Available online: http://tree.bio.ed.ac.uk/software/figtree/ (accessed on 19 January 2018).
60. Granmo, A. Morphotaxonomy and Chorology of the Genus *Hypoxylon* (Xylariaceae) in Norway. *Sommerfeltia* **1999**, *26*, 1–81.
61. Stadler, M.; Fournier, J.; Beltrán-Tejera, E.; Granmo, A. The "red Hypoxylons" of the temperate and subtropical Northern Hemisphere. *N. Am. Fungi* **2008**, *3*, 73–125.
62. Stadler, M.; Fournier, J. Pigment chemistry, taxonomy and phylogeny of the Hypoxyloideae (Xylariaceae). *Rev. Iberoam. Micol.* **2006**, *23*, 160–170.
63. Stadler, M.; Fournier, J.; Quang, D.N.; Akulov, A.Y. Metabolomic studies on the chemical ecology of the Xylariaceae (Ascomycota). *Nat. Prod. Commun.* **2007**, *2*, 287–304.
64. Hennings, P. Fungi mattogrossenses a Dr. R. Pilger collecti 1899. *Hedwigia* **1900**, *39,* 134–139.
65. Wibberg, D.; Stadler, M.; Lambert, C.; Bunk, B.; Spröer, C.; Rückert, C.; Kalinowski, J.; Cox, R.J.; Kuhnert, E. High quality genome sequences of thirteen Hypoxylaceae (Ascomycota) strengthen the phylogenetic family backbone and enable the discovery of new taxa. *Fungal Divers.* **2021**, *106*, 7–28.
66. Kuhnert, E.; Surup, F.; Herrmann, J.; Huch, V.; Müller, R.; Stadler, M. Rickenyls A-E, antioxidative terphenyls from the fungus *Hypoxylon rickii* (Xylariaceae, Ascomycota). *Phytochemistry* **2015**, *118*, 68–73.
67. Kuhnert, E.; Navarro-Muñoz, J.C.; Becker, K.; Stadler, M.; Collemare, J.; Cox, R.J. Secondary metabolite biosynthetic diversity in the fungal family Hypoxylaceae and *Xylaria hypoxylon*. *Stud. Mycol.* **2021**, *99*, 100118.
68. Leman-Loubiere, C.; Le, G.G.; Debitus, C.; Ouazzani, J. Sporochartines A-E, a new family of natural products from the marine fungus *Hypoxylon monticulosum* isolated from a *Sphaerocladina sponge*. *Front. Mar. Sci.* **2017**, *4*, 1–9.
69. Surup, F.; Kuhnert, E.; Lehmann, E.; Heitkämper, S.; Hyde, K.D.; Fournier, J.; Stadler, M. Sporothriolide derivatives as chemotaxonomic markers for *Hypoxylon monticulosum*. *Mycology* **2014**, *5*, 110–119.
70. Surup, F.; Kuhnert, E.; Böhm, A.; Pendzialek, T.; Solga, D.; Wiebach, V.; Engler, H.; Berkessel, A.; Stadler, M.; Kalesse, M. The rickiols: 20-, 22-, and 24-membered macrolides from the ascomycete *Hypoxylon rickii*. *Chem. Eur. J.* **2018**, *24*, 2200–2213.
71. Ma, H.X.; Vasilyeva, L.; Li, Y. *Hypoxylon* from China-2: *H. dengii* sp. nov and *H. crocopeplum* new to China. *Mycotaxon* **2012**, *122*, 1–5.